# COMPARISION OF CONTROL STRUCTURES FOR A BIDIRECTIONAL HIGH-FREQUENCY DC-DC-CONVERTER

Felix A. HIMMELSTOSS, Johann W. KOLAR and Franz C. ZACH

Technical University of Vienna - Power Electronics Section
Gusshausstrasse 27-29, A - 1040 Vienna, AUSTRIA

## A B S T R A C T

A system for DC-DC power conversion based on a buck-boost converter topology is presented which makes power flow in both directions possible. The possibility of bidirectional power flow is useful for certain applications, such as uninterruptable power supplies (UPS). Starting from a structure diagram the transfer function of the system is derived. The controller for the converter is then realized as simple voltage controller , as voltage controller with an inner loop current controller (cascade-control) and with two kinds of state-space control. The transfer functions of the different system parts are derived and dimensioning guidelines for the controller sections are presented. The closed-loop behavior of the bidirectional converter for the different control-structures is analyzed based on simulation using duty-cycle averaging; bode-diagrams and step responses are shown for a characteristic example.

## 1. INTRODUCTION

Unidirectional converters in their basic configuration are characterized by an asymmetrical structure regarding their topology and/or regarding their controllability. Switching instants and conduction intervals of the diodes on the secondary are - dependent on the converter topology (buck or boost converters etc.) - determined indirectly by changing the switching status of the power transistor on the primary.

An intrinsic limitation of this concept is given by the direction of current and energy flow (first quadrant of the current-voltage phase plane) which is determined by the direction of the electric valves.

Bidirectional power flow between constant voltage (current) sources requires replacement of the unidirectional power semiconductor devices by an antiparallel combination of a directly (power transistor) and an indirectly (diode) controllable electrical valve. This results in a unidirectionally controllable power semiconductor. However, this requires fixed voltage polarity, equivalent to restriction to the first and second quadrants of the current-voltage plane.

The application of this general concept to a buck-boost converter structure leads to a topology with a remarkably simple topology. For further details of the converter structure see [1].

The stationary system condition is characterized by a time constant average energy content of the primary and secondary electrical and magnetic energy storage devices. This equilibrium between energy input and output corresponds to a duty ratio defined only by the voltage ratios (and turns ratios) of primary and secondary independent of the energy flow direction. This is shown in [1,2]. Idealized components are assumed and the push-pull control of transistors $T_1$ and $T_2$ is applied as indicated in Fig.1.

Continuous operation is given if the transistor on the primary is turned on again before $i_{d2}$ reaches zero.

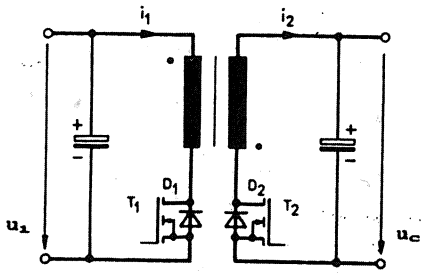


Fig.1. Bidirectional converter with push-pull control (principal)

## 2. MODEL REPRESENTATION OF THE BIDIRECTIONAL CONVERTER

For the derivation of the model equations for the bidirectional converter compare [1,2]. Parasitic elements considered are the (ohmic) resistances on the primary and secondary $R_1$, $R_2$ (consisting of the sums of the winding resistances and the $R_{Dson}$ of the semiconductor switches).

For different load cases (ohmic load, current or voltage sources, loads with constant power consumption - all for the primary and/or secondary side) one can establish two describing differential equation systems for closed switch and for

open switch on the primary. These two systems can be combined into one system of differential equations if one assumes switching periods small compared to the system time constants. Then the system of nonlinear differential equations is linearized about its operating point.

As an example we consider the results for the U-R operation, i.e. where a voltage source is on the primary side and an ohmic load is on the secondary side (Eqs.3,4). A closer investigation shows that the basic form of the transfer function (but, of course, not the coefficients) is equal for ohmic loads, for loads with constant current consumption and for loads with constant power consumption. This is also independent whether the load is on the primary or on the secondary side. The form of the transfer function between duty cycle and converter output voltage is given by

$$G_{u\alpha}(s) = \frac{s\cdot z_1 + z_0}{s^2 + s\cdot n_1 + n_0} \quad . \tag{1}$$

For coupling of two rigid DC voltage systems we receive a simpler transfer function for the relationship between duty cycle and converter current of the following form:

$$G_{i\alpha}(s) = \frac{z_0}{s + n_0} \quad . \tag{2}$$

Thereby $n_0$ is determined by the parasitic system resistances. Because $n_0$ is usually small, this means that the system basically forms an integrator.

The system equations for U-R operation are (cf.[2]):

$$\begin{bmatrix} \frac{d(\hat{u}_c)}{dt} \\ \frac{d(\hat{i}_1)}{dt} \end{bmatrix} = \begin{bmatrix} A_{11} & A_{12} \\ A_{21} & A_{22} \end{bmatrix} \cdot \begin{bmatrix} \hat{u}_c \\ \hat{i}_1 \end{bmatrix} + \begin{bmatrix} B_{11} \\ B_{21} \end{bmatrix} \cdot \hat{\alpha} \tag{3}$$

with

$$A_{11} = -\frac{1}{R_0\cdot C}\ , \quad A_{12} = (1-\alpha_0)\cdot\frac{N_1}{C\cdot N_2}\ , \tag{4a}$$

$$A_{21} = -\frac{1-\alpha_0}{L_2}\cdot\frac{N_2}{N_1}\ , \tag{4b}$$

$$A_{22} = -\left[\alpha_0\cdot\frac{R_1}{L_1} + (1-\alpha_0)\cdot\frac{R_2}{L_2}\right], \tag{4c}$$

$$B_{11} = -\frac{I_{10}\cdot N_1}{C\cdot N_2}\ , \tag{4d}$$

$$B_{21} = \frac{U_{10}}{L_1} + \frac{U_{c0}\cdot N_2}{L_2\cdot N_1} + \left[\frac{R_2}{L_2} - \frac{R_1}{L_1}\right]\cdot I_{10}\cdot \tag{4e}$$

This leads to the following structural diagram (Fig.2):

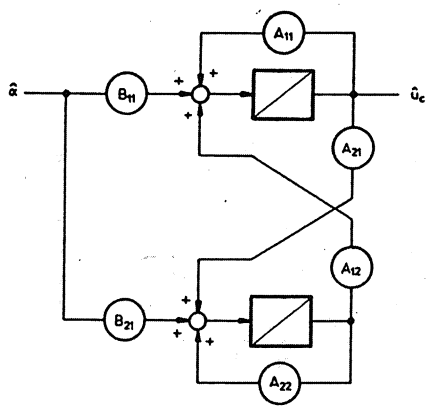


Fig.2. Structural diagram of the linearized bidirectional push-pull converter

The relationships for the stationary case result from [2]:

$$\frac{1}{C}\cdot\frac{N_1}{N_2}\cdot I_{10}\cdot(1-\alpha_0) - \frac{U_{c0}}{R\cdot C} = 0 \tag{5}$$

$$\frac{R_2}{L_2}\cdot(\alpha_0-1)\cdot I_{10} + \frac{N_2}{N_1\cdot L_2}\cdot(\alpha_0-1)\cdot U_{c0} + (U_{10}+R_1\cdot I_{10})\cdot\frac{\alpha_0}{L_1} = 0 \tag{6}$$

In the operating point (given by $U_{10}$, $U_{c0}$, $I_{10}$ and $\alpha_0$) we can calculate the transfer function between output voltage $u_c$ and the duty ratio $\alpha$ from Eq.(3).

We receive $\hat{u}_c(s) = G_{u\alpha}(s)\cdot\hat{\alpha}(s)$ (7)

where

$$G_{u\alpha}(s) = \frac{s\cdot B_{11} + A_{12}\cdot B_{21} - A_{22}\cdot B_{11}}{s^2 - s\cdot(A_{11}+A_{22}) + \det A} \quad . \tag{8}$$

## 3. SINGLE LOOP CONTROL

By linearization in the operating point the system of nonlinear equations has been transformed into a linear one (Eq.3).

Therefore it has been possible to give a transfer function of the bidirectional converter (Eq.8). Now it is possible to use the means of controller dimensioning for linear systems. One has to keep in mind, however, that the controller based on the dimensioning really works as designed only in the chosen operating point.

### 3.1 Pole-Zero-Diagram

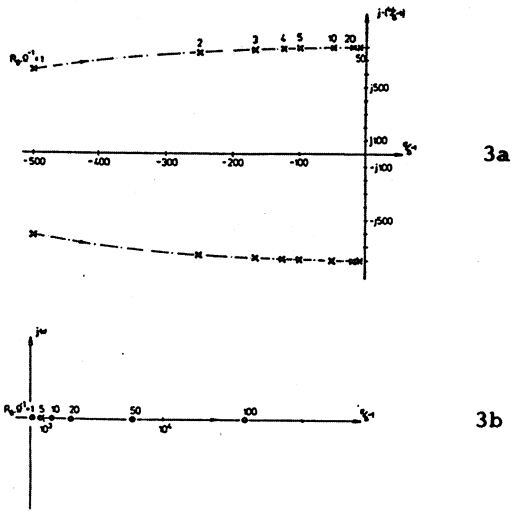


Fig.3 a) Pole locations, b) Zero locations for a bidirectional converter.

In order to cover the operating behavior for varying operating points one has to determine pole-zero-diagrams for a representative number of different operating points. Fig. 3a shows the pole locations for a small experimental converter in dependency on the load. For lower load the poles come closer to the vertical axis and therefore the system becomes less damped. Fig. 3b shows the locations of the zero for the same converter. The zero always lies in the right half plane and moves to the right for reduced load.

### 3.2 Bode Plot of the Controlled System

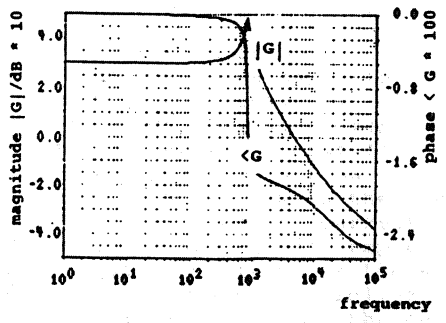


Fig.4. Bode plot of the converter

Fig. 4 shows the Bode plot of the bidirectional converter. Now one can base the controller dimensioning on the Bode plot [4,pp.168-207]. This results in a PI(proportional-integral)controller. One can show [2] that the controller gain is dependent very much on the converter load. On the other hand, the integration time constant remains almost constant. The Bode plot for the open control loop is shown in Fig. 5. The controller has to be dimensioned for the worst case. Here, this would be for the least damping of the controlled system.

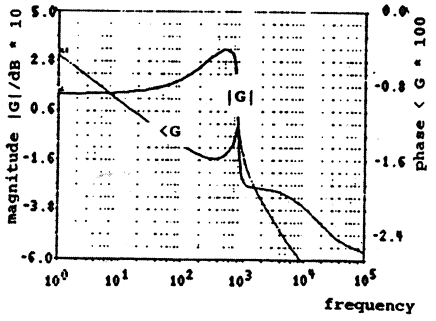


Fig.5. Bode plot for the open control loop

### 3.3 Bode Plot of the Closed Loop

The Bode plot (Fig.6) shows the closed loop system behaviour for reference value changes . However, for application as converter for constant output voltage the behaviour relative to load changes (disturbance frequency response) is decisive.

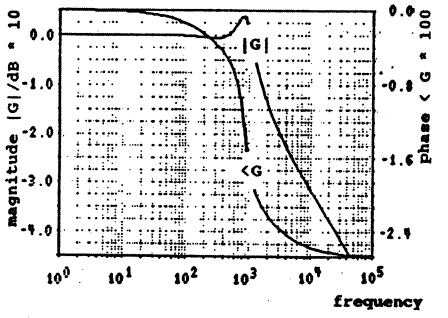


Fig.6. Bode plot for the closed loop

### 3.4 System Step Response

The research in [2] has shown that the control quality of a single loop voltage control cannot meet higher standards. Damping of the system basically is given by the load. Stability considerations have shown very unfavorable positions of the system poles and zeros. The controller such dimensioned is only applicable for a limited operating region.

## 4. THE BIDIRECTIONAL CONVERTER WITH CASCADE CONTROL

### 4.1 Partial transfer functions

Dividing the overall transfer function (Equ.3) into two partial transfer functions ($G_{ua}(s)=G_{ia}(s)\cdot G_{ui}(s)$) makes it possible to design a two loop control stucture (Fig.7). Thereby $G_{ia}(s)$ represents the relationship between the duty ratio and the converter current and $G_{ui}(s)$ gives the relationship between converter current and output voltage.

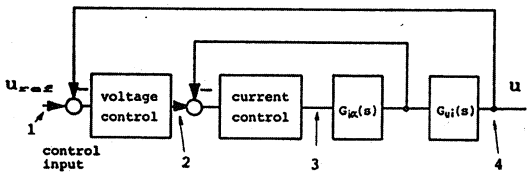


Fig.7. Cascade control structure

The state vector representation is

$$\dot{x} = A\cdot x + B\cdot u \qquad (9a)$$
$$y = C\cdot x + D\cdot u \qquad (9b)$$

where Eq.(9a) is defined by Eq.(3) where matrix B is a vector b; in Eq(9b) matrix C is reduced to a vector c and matrix D is reduced to a scalar.

Now we can (according to [4,p.300]) determine the transfer function as

$$G(s) = c^T\cdot(s\cdot I - A)^{-1}\cdot b + d \qquad (10)$$

For the determination of the transfer function $G_{ia}$ (which gives the relationship between converter current $i_1$ and the duty ratio $\alpha$), we have $c^T=(0,1)$ and $d=0$ ( Eq. (9b) -the output equation- is reduced to $y=i_1$). This results in (detA cf. Eq.(14)):

$$G_{ia}(s) = \frac{s\cdot B_{21} + A_{21}\cdot B_{11} - A_{22}\cdot B_{11}}{s^2 - s\cdot(A_{11}+A_{22}) + detA} \qquad (11)$$

The relationship between output voltage $u_c$ and converter current $i_1$ is given by

$$G_{ui}(s) = \frac{s\cdot B_{11} + A_{12}\cdot B_{21} - A_{22}\cdot B_{11}}{s\cdot B_{21} + A_{21}\cdot B_{11} - A_{11}\cdot B_{21}} \qquad (12)$$

The overall transfer function of the converter system now has been split into two partial transfer functions. Now one can design a controller for the current control section and thereby stabilize the inner loop. The transfer function resulting from this now together with the relationship between converter current and output voltage $G_{ui}(s)$ (Eq.12) represents the section to be controlled for the voltage control. The voltage controller now can be designed separately. For the design we can apply now all means for the control design for linear systems (see, e.g., [4]). For the application of cascade control for conventional SMPS there exist numerous references ( e.g., [7]).

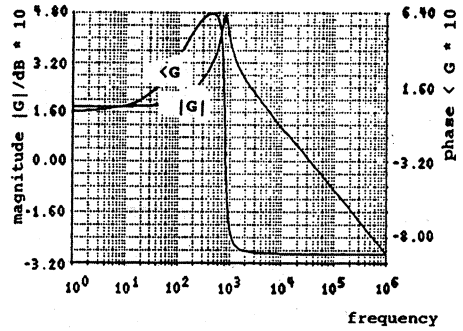


a) $G_{ia}(s)$

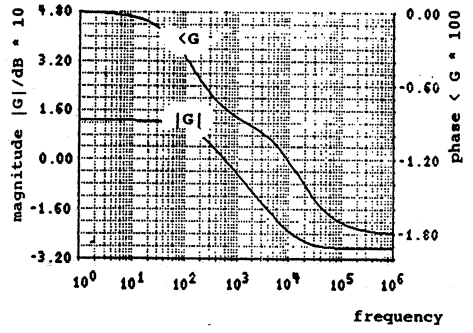


b) $G_{ui}(s)$

Fig.8. Bode diagrams for the partial transfer functions a)$G_{ia}(s)$, b)$G_{ui}$

### 3.2 Inner Contol Loop - Inner Loop Current Controller

Design of the P (proportional) controller: The transfer function (between points 2 and 3 in Fig.7) of the current control loop results in

$$G_{iP}(s)=K_P\cdot\frac{B_{21}\cdot s+A_{21}\cdot B_{11}-A_{11}\cdot B_{21}}{s^2+s\cdot(-A_{11}-A_{22}+K_P\cdot B_{21})+detA+K_P\cdot bc} \qquad (13)$$

with $detA = A_{11}\cdot A_{22} - A_{21}\cdot A_{12}$

$$ab = A_{21}\cdot B_{11} - A_{11}\cdot B_{21} \qquad (14)$$

$$bc = A_{12}\cdot B_{21} - A_{22}\cdot B_{11}$$

and $K_P$ as the amplification of the P-controller.

As shown in [5] it is not necessary to use PI control or higher order control for the inner loop.

### 4.3 The Outer Control Loop - the Voltage - Control

In a second step now an outer loop voltage control will be designed. Dependent on the current control realization we receive different systems to be controlled for the voltage controller.

The transfer function (between points 2 and 4 in Fig.7) of the controlled system for voltage control with inner loop P. current control circuit is:

$$G_u(s)=K_P\cdot\frac{B_{11}\cdot s+A_{12}\cdot B_{21}-A_{22}\cdot B_{11}}{s^2+s\cdot(-A_{11}-A_{22}+K_P\cdot B_{21})+\det A+K_P\cdot ab} \quad (15)$$

As shown in [5] a PI control for the outer loop is sufficient.

The transfer function for a PI-controller is

$$G_{uPI}(s) = \frac{K_{Iu}\cdot(1+s\cdot T_{Iu})}{s\cdot T_{Iu}} \quad (16)$$

## 4.4 Transfer Function for the Overall System

For the overall system the following transfer function (between points 1 and 4 in Fig.7) results for a PI-voltage-controller with P-current-controller

$$G(s) = \frac{\delta_2\cdot s^2 + \delta_1\cdot s + \delta_0}{\mu_3\cdot s^3 + \mu_2\cdot s^2 + \mu_1\cdot s + \mu_0} \quad (17)$$

$$\begin{aligned}
\text{with } \delta_2 &= K_{Iu}\cdot K_{Ii}\cdot B_{11}\cdot T_{Iu}\\
\delta_1 &= K_{Iu}\cdot K_{Ii}\cdot(B_{11} + T_{Iu}\cdot bc)\\
\delta_0 &= K_{Iu}\cdot K_{Ii}\cdot bc\\
\mu_3 &= T_{Iu}\\
\mu_2 &= T_{Iu}\cdot(-A_{11} - A_{22} + K_P\cdot B_{21}) + K_{Iu}\cdot K_{Ii}\cdot B_{11}\cdot T_{Iu}\\
\mu_1 &= T_{Iu}\cdot(\det A + K_P\cdot ab) + K_{Iu}\cdot K_{Ii}\cdot(B_{11} + T_{Iu}\cdot bc)\\
\mu_0 &= K_{Iu}\cdot K_{Ii}\cdot bc
\end{aligned} \quad (18)$$

The controller design was performed with the means of the classical linear control theory. For the practical design we have to consider the limitations of the duty ratio and of maximum permissible transformer (converter) current, however. The controller parameters therefore have to be checked for their validity.

## 4.5 System step response

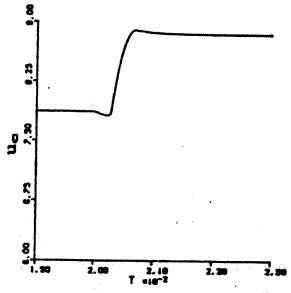

Fig.9. Closed loop response for the PI-P-structure

Fig.9 shows the closed loop step response calculated based on the nonlinear model for a PI-voltage-controller with a P-current-controller . With the PI-PI structure the performance cannot be improved significantly.

The research has shown that the cascade control results in a substantially better control behavior (as compared to the single loop control) because it is possible to stabilize the two loops then very efficiently.

# 5. STATE-SPACE-CONTROLLER

## 5.1 Simple state space controller

Another possibility to attain a good closed loop response is to realize a state-space controller. An examination of the simple state space control structure (Fig.10) shows that this structure only has limited applicability to the control of the bidirectional converter. The prefilter can only be dimensioned exactly if the knowledge of the system is very good. However, the nonlinearity of the system leads to a prefilter which can successfully be applied only in a small region around the operating point. A small deviation from the operating point leads to an undesired stationary control error. Therefore a fourth concept is investigated in section 5.2.

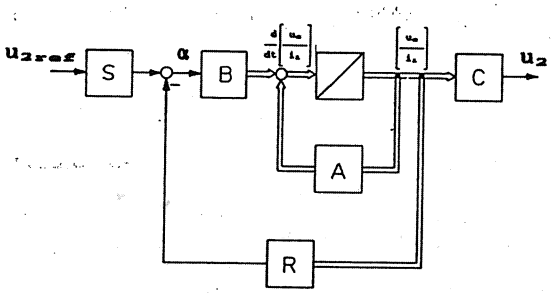


Fig.10. Simple State Space Control Structure (for A, B see Eq.(9a), R Controller matrix, C becomes $c^T=(1,0)$

## 5.2 Extended state space control

Taking the control error as another state variable [6] we receive an extended state space control structure (Fig.11). This leads to very satisfactory operating conditions.
Starting with the system equations (Eq.-(3)) one can determine the elements of the controller matrix according to [6]. Thereby the pole locations are chosen:

$$\begin{aligned}
s_1 &= \sigma_1 + j\cdot\Omega\\
s_2 &= \sigma_1 + j\cdot\Omega\\
s_3 &= \sigma_2
\end{aligned} \quad (19)$$

with $\sigma_1, \sigma_2 < 0$.

A rather lengthy calculation leads to the

elements of the controller, described by (1x3) matrix here. (The practical realization of the controller only requires an adder circuit with an operational amplifier - the real practical problem here as well as for the cascade control lies in the exact and disturbance free measurement of $i_1$).

$$r_{12} = \frac{[m_2+\sigma^2+\Omega^2+2\cdot\sigma_1\cdot\sigma_2+q_{23}/q_{33}\cdot(\sigma_1^2\cdot\sigma_2+\Omega^2\cdot\sigma_2)]\cdot q_{11}-[m_1-2\cdot\sigma_1-\sigma_2]\cdot q_{21}}{q_{11}\cdot q_{22}-q_{21}\cdot q_{12}}$$

$$r_{11} = \frac{[m_1-2\cdot\sigma_1-\sigma_2]\cdot q_{22}-[m_2+\sigma^2+\Omega^2+2\cdot\sigma_1\cdot\sigma_2+q_{23}/q_{33}\cdot(\sigma_1^2\cdot\sigma_2+\Omega^2\cdot\sigma_2)]\cdot q_{12}}{q_{11}\cdot q_{22}-q_{21}\cdot q_{12}} \qquad (20)$$

$$r_{13} = -\frac{(\sigma_1^2\cdot\sigma_2+\Omega^2\cdot\sigma_2)}{q_{33}}$$

with the abbreveations

$$q_{11} = B_{11} \qquad q_{12} = B_{21}$$

$$q_{21} = -A_{22}\cdot B_{11} - B_{21}\cdot A_{12}$$

$$q_{22} = -A_{11}\cdot B_{21} + A_{21}\cdot B_{11}$$

$$q_{23} = -B_{11} \qquad q_{33} = -A_{12}\cdot B_{21} + A_{22}\cdot B_{11}$$

$$m_1 = A_{11} + A_{22} \qquad (21)$$

$$m_2 = -A_{11}\cdot A_{22} + A_{21}\cdot A_{12}$$

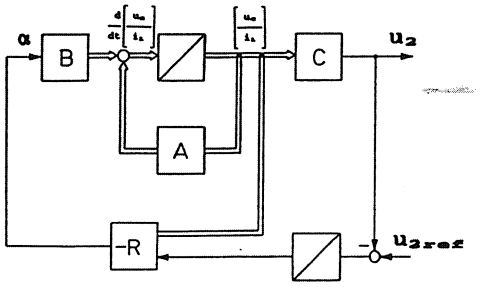


Fig.11. Extended State Space Control Structure (for A,B,C,R see Fig.10)

4.3 System step response

The advantage of the state space approach (as given here) is that the system behavior can be chosen to a large extent by selection of the pole positions (Eq.(19)). One has to keep in mind, however, that, e.g. the values of $\sigma$ and $\Omega$ have to be selected such that the limitations of the state and controller variables are not reached. Such limitations are, e.g., given by the maximum transistor currents, by core saturation, by the fact $\alpha<0$ and $\alpha>1$ could be calculated by the controller but are not physically realizable etc.

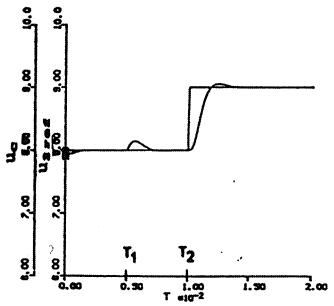


Fig.12. System step response to load change at $T_1$ and reference value change at $T_2$

## 6. CONCLUSIONS

This paper has shown the controller design for a bidirectional buck-boost-converter. Dimensioning guidelines have been given for controller structures with one loop control, with two loop (cascade) control and for state space control. The system behavior has been investigated for all these cases. It has been shown that the one loop control does not yield satisfactory results. The cascade control and the state space control, however, lead to very good control behavior. This concerns the stability, as well as the dynamic quality (such as fast control response).

## 7. REFERENCES

[1] Kolar,J.W.,Himmelstoss,F.A., and Zach, F.C.:"Analysis of the Control Behavior of a Bidirectional High-Frequency DC-DC-Converter", PCIM 88, Munich May 8-10,1988,pp.344-359

[2] Himmelstoss,F.A.,Kolar,J.W., and Zach, F.C.:"Analysis of Closed-Loop Control Behavior of a Bidirectional High Frequency DC-DC Converter", PCIM 88, Tokio Dec 8-10,1988,pp.174-184

[3] Middlebrook,R.D.,Cuk,S.: "Advances in Switched-Mode Power Conversion, Vol.1, Pasadena:Teslaco,1981

[4] Föllinger,O.: "Regelungstechnik", Heidelberg:Hüthig Verlag.1984

[5] Himmelstoss,F.A.,Kolar,J.W., and Zach, F.C.:"Analysis of the Cascade-Control Behavior of a Bidirectional High Frequency DC-DC Converter",HFPC 89,Naples Fl., May 14-18,1989

[6] Weinmann,A.:"Regelungstechnik", Vol.3, Wien: Springer Verlag,1986

[7] Kawabata T. et al: "Chargerless UPS Using Multi-functional BIMOS Inverter", IEEE IAS Annual Meeting 1986, pp.513 - 520.

**ACKNOWLEDGEMENT**

The authors are very much indebted to the Austrian «Fonds zur Förderung der wissenschaftlichen Forschung» who supports the work of the power electronics section at their university.